frontiers in Energy Research

TYPE Original Research
PUBLISHED 01 April 2026
DOI 10.3389/fenrg.2026.1659609

OPEN ACCESS

EDITED BY
Simeone Chianese,
University of Campania Luigi Vanvitelli, Italy

REVIEWED BY
Yunzhi Chen,
National Renewable Energy Laboratory (DOE), United States
Wenhao Jia,
Xi'an Jiaotong University, China
Mark Ruth,
National Renewable Energy Laboratory (DOE), United States

*CORRESPONDENCE
Abdallah Nour El Din,
a.noureldin@tudelft.nl

RECEIVED 04 July 2025
REVISED 11 February 2026
ACCEPTED 23 February 2026
PUBLISHED 01 April 2026

CITATION
Nour El Din A, Verzijlbergh RA and De Vries LJ (2026) Exploring the trade-offs among flexibility options in hydrogen production .
Front. Energy Res. 14:1659609.
doi: 10.3389/fenrg.2026.1659609

Exploring the trade-offs among flexibility options in hydrogen production

Abdallah Nour El Din*, Remco A. Verzijlbergh and Laurens J. De Vries

Faculty of Technology, Policy and Management, Delft University of Technology, Delft, Netherlands

Due to the steady increase in renewable energy capacities, future power systems are expected to exhibit flexibility at different timescales. Demand-side response and energy storage are two key elements for providing this flexibility. In this paper, we analyze how a large energy consumer with flexibility options interacts with the energy system. In this context, the interaction is not only limited to the operational aspect, but also extends to investment decisions in flexibility options. To perform this analysis, a simple power system model is considered, coupled with a grid-connected electrolysis plant and storage facility. Then, a linear programming problem is solved to optimize the energy costs as well as the investment costs of hydrogen facilities. For this analysis, a new mapping method for near-optimal regions is formulated and implemented. This implementation enables an extended sensitivity analysis, where the evolution of the near-optimal region is analyzed rather than the evolution of the optimal point. Finally, an abstract definition of flexibility in hydrogen consumption is presented, and its influence is interpreted. The results indicate that varying power system settings lead to distinct patterns of investment in flexibility capacities. In addition, they emphasize the complementary relationship between flexible consumption and the need for storage.

KEYWORDS
hydrogen, energy storage, power system flexibility, near-optimal solutions

1 Introduction

1.1 Motivation

As the world faces increasing pressure to address climate change, reducing greenhouse gas emissions has become an inevitable choice for securing a sustainable future. In addition to the ongoing transition in the energy sector, industrial decarbonization is an inevitable step toward achieving carbon neutrality goals. This results in a higher contribution of electricity to industrial primary energy consumption. There is potential for synergy through flexible industrial operations and the deployment of storage facilities for synthetic fuels, particularly in the context of indirect electrification. The study of flexibility potentials for a large consumer is not limited to operational analysis, where the consumer schedules their demand based on energy prices. It also includes studying investments in flexibility. In the case of indirect electrification, there is a need for investment in energy conversion and energy storage facilities.

To perform this analysis, an optimization problem is defined. This problem combines a power system element and a flexible demand element. This problem

aims to minimize the total cost of energy generation over a sample year and the annualized investment cost in flexibility facilities. The capacities of flexibility facilities will then be optimized under operational constraints of the power system and the flexible consumption. Note that the primary research outcome is not the values of the optimal investment, but rather how this optimal value responds to variations in selected optimization problem variables. In other words, the focus is on the sensitivity of the optimal investment to the system conditions rather than the investment figure.

1.2 Problem definition

The electric energy required for decarbonized iron ore reduction in the Netherlands serves as a source of flexibility in the formulated problem. In this problem, an on-grid electrolysis facility and a hydrogen storage facility maintain a constant flow rate of hydrogen required for the reduction process. On the other hand, the flexible operation of the electrolysis facility allows it to respond to the power system and thus schedule its electric demand accordingly. Due to the scale of the electrolyzer, its operation influences the wholesale prices of electricity. In short, the formulated problem aims to optimize the capacities of electrolysis and storage facilities under two dynamic constraints: the hydrogen flow rates between the electrolyzer, storage, and the steel plant, and the electrolyzer's impact on the energy market.

1.3 Literature review

The co-optimization of hydrogen systems within high-renewable power grids has been studied from multiple perspectives in the literature, including green hydrogen production and transportation, storage, and safety considerations (Jia et al., 2026; Haoxin et al., 2025). Beyond technology-specific analysis, the insights of such studies depend strongly on the detail level of the modeled systems.

The derivation of the model for the defined system is an essential step in this research. In this step, a research decision must be made: What level of detail should be applied? Here, there is a trade-off between the accuracy of representation on one hand and the simplicity of the optimization problem and its applications on the other. In the following subsection, we present a review of the detail-level decisions in previous works.

1.3.1 Detail levels

Research efforts have been conducted to study the economic performance of a decarbonized steel industry. In (Boldrini et al., 2022), A. Boldirini et al. formulated a model of an exemplary steel plant. Then, after utilizing a historic time series of electricity from the Dutch day-ahead market, a linear programming problem was solved to minimize the cost of the plant's electricity consumption. This provides insight into the market price's influence on the plant's operation. Other research efforts focused on creating models with a higher level of detail. A. Kruger et al. studied the economics of iron ore reduction with hydrogen using water electrolysis technologies. The authors considered different electrolysis technologies. The sensitivity of the process economics to the electrolyzer's capital expenditure (CAPEX) and electricity costs was then analyzed (Krüger et al., 2020). X. Zang et al. studied the operation of a steel plant that is composed of four main processes (Zhang et al., 2016). The scheduling problem was created using resource task network modeling. This method enabled the application of operational constraints between each of the four processes. The high level of detail in this resulted in a high computational cost. The potential of industrial demand response was studied for other industries. In (Sofana Reka and Ramesh, 2016), the authors studied the demand response of a refinery using the resource network modeling approach. S. Valera et al. investigated the scheduling of alkaline water electrolysis for power-to-X applications (Varela et al., 2021). Researchers used a data-driven approach to analyze the scheduling of an air separation unit in (Tsay et al., 2019).

On the other hand, some researchers focused on implementing aggregate models to study the influence of flexibility. An available flexible industrial demand model is characterized by two terms: α, T^{proc}. The first term, ranging between 0 and 1, represents the extent of industrial demand flexibility. The second term, denoted as the process horizon, is used as a time horizon to ensure that the industrial demand redistribution is energy neutral. Other modeling choices were also explored (Papadaskalopoulos et al., 2018). Another approach to representing industrial demand is to divide it into three options. The flexible demand option allows customers to reschedule their demand within operational constraints. The second option is on-site generation, where the customer can run their on-site backup generator. The final option is energy storage, where the customer purchases and stores energy during periods of low prices (Angizeh et al., 2019).

It can be concluded that the two modeling approaches serve different purposes. The high-level approach examines the operational challenges of flexible energy consumption and the potential benefits from the plant's perspective, assuming the market price is given. In contrast, low-level models are used to explore the benefits at the system level without considering the constraints imposed by the plant's dynamics. This review shows that modeling with a moderate level of detail has not been addressed. This level would enable us to optimize investment in flexibility capacities, consider the impact of demand response on the energy market, and provide a representation of scheduled hydrogen flows that meet the hydrogen demand.

1.3.2 Optimization analysis

Aside from single-point optimization, performing a near-optimal analysis helps provide a better understanding of solution behavior. In the near-optimal analysis, the objective function value is allowed to deviate from the optimal value within a defined range, known as the optimality gap. This variation enables us to explore different optimization paths, or different sets of optimization variables that result in a near-optimal result. This practice is common in energy system analysis, especially when studying energy storage and flexibility (Pedersen et al., 2021; Teo et al., 2018; Pandzic et al., 2015; Neumann and Brown, 2021; Grochowicz et al., 2023). In addition, modeling to generate alternatives is used to examine the influence of different design and policy choices for energy system analysis (Lombardi et al., 2020; Lombardi et al., 2023). This is due to the shortcomings of optimal solution analysis, including the imperfect representation of the

mathematical models, the variability of problem constraints (such as fuel costs and weather conditions), and the lack of information on the solution's robustness (Voll et al., 2015).

What appears to be missing in the literature is a systematic study of the impact of power system parameters on the trade-offs between flexibility options for hydrogen production and a method that is not sensitive to small variations in problem settings. In this research, near-optimal analysis is employed to explore various options for near-optimal electrolysis and storage capacities, as well as near-optimal investment options.

1.4 Research scope

1.4.1 Research methodology

The purpose of this research is to investigate the interactions between large energy consumers and the power system. Mainly, the focus is on the optimal investment and how it responds to variations in the problem variables. The analysis results are relevant to both industry and energy system planners.

Figure 1 describes the model used for this paper. The two shaded rectangles represent the two main components of the model: the power system, depicted in blue, and the hydrogen flow, shown in green. The electrolysis plant is a common component of the two parts: its level of operation influences electricity prices and determines the quantity of hydrogen that can be generated, stored, or fed directly to the reduction process. Additionally, the model takes into account the energy required for hydrogen compression during storage. This model is used to run an optimization problem that minimizes the system cost. The system cost is composed of two components: the generation cost of the power plants and the annualized costs of investment in the hydrogen facilities. This enables us to investigate the impact of variables on the optimal hydrogen capacities. In other words, how do the CAPEX of electrolysis and storage, the natural gas price, the carbon emission price, or the renewable capacities impact the optimal investments in electrolysis and storage capacities?

1.4.2 Proposed contributions

This paper presents the development of a model of an optimization problem that couples the operation of the power system with a large flexible energy consumer. This enables us to examine the impact of the exhibited flexibility on the energy market. In addition, to understand the interactions among the optimization problem variables, this paper includes an analysis of the interactions between the power system variables and the optimal capacities for storage and electrolysis. Finally, in this paper, the convexity attribute of the linear optimization problem is utilized to map the near-optimal regions. The mapping process has two merits. The first merit is that it allows for a better understanding of the problem solution. The shape of the region describes the implicit relation between the two capacities, storage and electrolysis. In addition, the application of near-optimal region mapping provides enhanced insight into the sensitivity of optimal capacities with respect to problem variables. Instead of conducting sensitivity analyses on the optimal capacity points, the study of variations in the near-optimal region generates an extended sensitivity analysis.

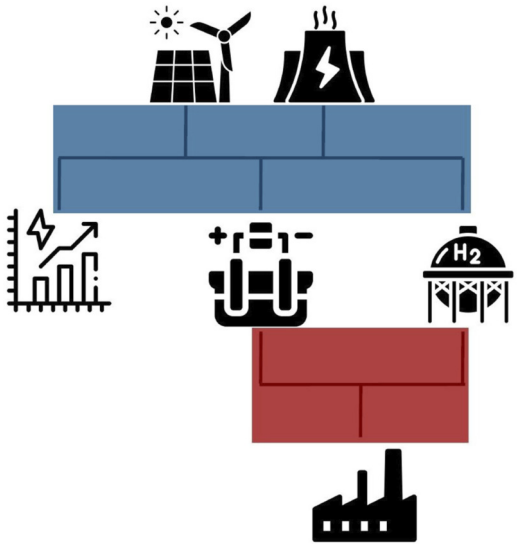

FIGURE 1
Visualization of the formulated model. The blue-shaded area represents the power system, illustrating the interactions among renewable resources, dispatchable generation, national electricity demand, electrolysis, and storage facilities. The red-shaded area depicts the hydrogen system, highlighting the interactions between the electrolysis plant, the storage plant, and the hydrogen demand.

1.5 Paper layout

In this paper, Section 2 outlines the steps required for developing the model. Section 3 then explains the simulation setup, including the sources of data and a description of the method used to map the near-optimal regions. In Section 4, the results of the optimization problem are presented and discussed. Finally, the paper's conclusions and recommendations are presented in Section 5.

2 Model development

Given the mutual influence between power generation and hydrogen flow dynamics, the simulation of the defined scenario is governed by a linear optimization problem. Within this problem, the hourly power generation, electrolysis operation, and hydrogen flow rates are optimized to satisfy the energy conservation constraints. In addition, the capacities of the electrolysis plant and hydrogen storage facility are optimized to minimize the system cost.

2.1 Objective function

The ultimate purpose of the optimization problem is to optimize operational and investment costs. Therefore, the objective function can be formulated as follows:

$$\min_{P_{g,t},K_S,K_E} \quad \sum_{g=1}^{G}\sum_{t=1}^{T} P_{g,t}\cdot MC_g + A_S\cdot C_S\cdot K_S + A_E\cdot C_E\cdot K_E \qquad (1)$$

The objective function, Equation 1, represents the total system cost to be minimized. The first term, representing the power generation costs, is the sum of all power generated for every unit, $P_{g,t}$

multiplied by its corresponding marginal cost of energy generation, MC_g. On the other hand, the two other terms account for the annualized investment costs of the storage and electrolysis facilities. These costs are obtained as the product of the annuity factor A, CAPEX C, and capacity K.

In addition to the variables present in the equation, the simulation includes other optimization variables, such as the storage level, the hydrogen consumption, and the hydrogen flow rates. Although these variables significantly influence the optimization problem, they do not contribute directly to the objective function.

2.2 Constraints

In this subsection, the constraints of the optimization problem are explained. These constraints are divided into three main categories: power system constraints, hydrogen constraints, and iron reduction constraints.

2.2.1 The power system

Equation 2 presents an energy balance constraint. The total energy generated by all conventional generation units $P_{g,t}$ and renewable resources $P_{res,t}$ is equal to the sum of the national electricity demand D_E, electrolysis power consumption $P_{E,t}$, and hydrogen compression energy consumption $P_{s,t}$ for every hour t.

$$\sum_{g=1}^{g=G} P_{g,t} + P_{res,t} = D_E + P_{E,t} + P_{s,t} \quad \forall t \tag{2}$$

In addition to energy conservation, the energy generated by every $P_{g,t}$ unit is limited to the unit's capacity K_g (Equation 3). In Equation 4, the renewable generation $P_{res,t}$ is bounded by the product of the installed renewable energy capacity K_{res} and the hourly capacity factor $CF_{res,t}$.

$$0 \le P_{g,t} \le K_g \quad \forall g, t \tag{3}$$

$$0 \le P_{res,t} \le CF_{res,t} \cdot K_{res} \quad \forall t \tag{4}$$

2.2.2 Hydrogen facilities

The upper and lower bounds, $LB \cdot K$ and $UB \cdot K$, of the electrolysis power consumption $P_{E,t}$ and the storage operating level $S_{l,t}$ are defined in Equations 5, 6.

$$LB_S \cdot K_S \le S_{l,t} \le UB_S \cdot K_S \quad \forall t \tag{5}$$

$$LB_E \cdot K_E \le P_{E,t} \le UB_E \cdot K_E \quad \forall t \tag{6}$$

Assuming a constant electrolysis efficiency η_E, the total amount of hydrogen generated at any given hour $G_{H_2,t}$ is defined as shown in Equation 7.

$$G_{H_2,t} = \eta_E \cdot P_{E,t} \quad \forall t \tag{7}$$

The excess generated hydrogen can be stored in the storage facility at any time step. In order to store hydrogen, energy is required for compression. Equation 8 describes the energy needed to compress hydrogen $P_{s,t}$ is a function of the storage efficiency η_S and the hydrogen inflow rate to the storage tank $F_{H_2,in,t}$.

$$P_{s,t} = (1 - \eta_S) \cdot F_{H_2,in,t} / \eta_E \quad \forall t \tag{8}$$

In addition, mass conservation equations applied to the hydrogen storage facility are described in Equation 9. The change in the hourly storage level $S_{l,t}$ is the integration of the difference between hydrogen inflow $F_{H_2,in,t}$ and outflow $F_{H_2,out,t}$ rates.

$$S_{l,t+1} - S_{l,t} = \Delta t \cdot \left(F_{H_2,in,t} - F_{H_2,out,t}\right) \quad \forall t \tag{9}$$

2.2.3 Hydrogen demand

This part of the model relates the hydrogen inflow rate to the storage and electrolysis facilities to the considered hydrogen demand. Two scenarios are considered for the hydrogen demand. In scenario one, the steel plant is assumed to operate constantly throughout the year. Therefore, as shown in Equation 10, the hydrogen demand $\bar{D}_{H_2}$ equals the hydrogen produced by the electrolyzer minus the inflow to the storage tank, plus the outflow from the storage tank.

$$\bar{D}_{H_2} = \left(G_{H_2,t} - F_{H_2,in,t}\right) + F_{H_2,out,t} \quad \forall t \tag{10}$$

In scenario two, another source of flexibility, operational flexibility, is considered. In this context, operational flexibility is defined as the ability to vary the consumption of hydrogen on an hourly basis. This requires overcapacity of the plant facility.

In this scenario, the capacity of the industrial plant is assumed to be oversized by a factor of $1 + \alpha$. Therefore, the hourly hydrogen demand $D_{H_2,t}$ can vary under the condition of meeting hydrogen demand quota over a defined time period, called a flexibility period d. The hydrogen hourly demand equations can be expressed as with Equations 11, 12:

$$D_{H_2,t} = \left(G_{H_2,t} - F_{H_2,in,t}\right) + F_{H_2,out,t} \quad \forall t \tag{11}$$

$$\sum_{t=1}^{t=d} \Delta t \cdot D_{H_2,t} = \bar{D}_{H_2} \cdot (d/\Delta t) \tag{12}$$

The flexible consumption can vary between the upper and lower bounds that depend on the over-sizing factor α, see Equation 13. Note that as the oversizing coefficient increases, the lower bound of consumption increases too.

$$LB_D \cdot (1 + \alpha) \cdot \bar{D}_{H_2} \le D_{H_2,t} \le (1 + \alpha) \cdot \bar{D}_{H_2} \quad \forall t \tag{13}$$

3 Simulation setup

To run an energy market optimization problem, power system data is needed. First, the capacities of the available generation technologies and historic time series of the national demand and renewable energy generation were collected from the ENTSOE Transparency Platform (ENTSO-E, 2023). Here, the national demand is used because the Netherlands is assumed

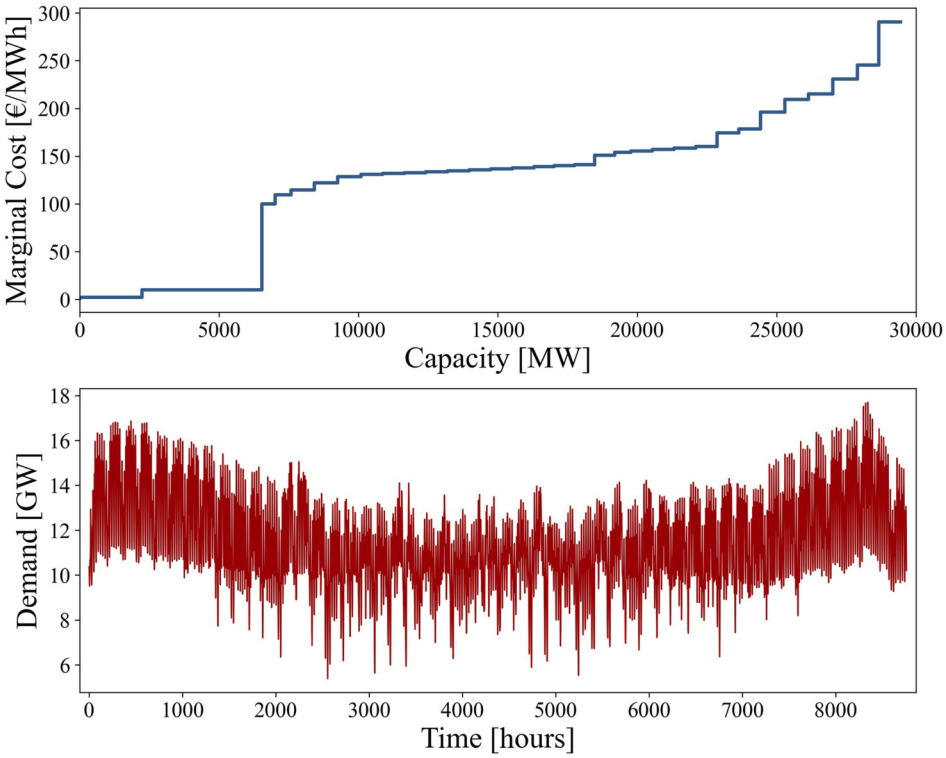

FIGURE 2
The merit order curve and the time series of the national demand of the Netherlands for the year 2022.

to be a closed system. Besides, the respective efficiencies of the generation units were collected (Corbie, 2024). Therefore, in addition to capacities in solar, wind, nuclear, and biomass, the model considers four coal generation units and 25 natural gas generation units. The resulting merit order is shown in Figure 2. The linear optimization problem was scripted in Python. The problem was solved using the Gurobi solver (Gurobi Optimization and LLC, 2023).

The values of the model variables are presented in Table 1. As shown in Table 1 and Equations 6, 7, the electrolyzer is modeled with a fixed efficiency and is assumed to operate continuously. This choice was motivated by two considerations. First, it allows the analysis to focus on the trade-offs between flexibility options, namely energy conversion and storage, rather than on technology-specific operating conditions. Second, it preserves computational tractability and convexity, which are essential for the region-mapping method.

Since the defined model results in a linear programming problem, the solution to this problem is always convex. This property can be used to map the near-optimal regions of the storage and electrolysis capacities. A near-optimal region represents the set of all feasible solutions that achieve an objective value within an acceptable margin of the optimum. In this study, this region is a two-dimensional space representing the feasible combinations of electrolysis and storage capacities.

To achieve this, the following steps are taken. First, the optimal solution is calculated $[C^*, E^*]$ and the optimal objective function value OF^* is stored. Then, a set of angles $[\theta_1, \theta_2, \ldots, \theta_n]$ on the optimization variables plane is selected. These angles are used to constrain the variation of the optimization variables within a predefined direction according to the Equations 14, 15:

$$C = C^* + k \cdot cos(\theta_i) \quad i \in [1, n] \tag{14}$$

$$E = E^* + k \cdot sin(\theta_i) \quad i \in [1, n] \tag{15}$$

TABLE 1 The values of model variables.

Model variable	Value	References
Electrolysis Efficiency [tonne/MWh]	0.02	
Storage efficiency [%]	96	Armstrong et al. (2022)
Natural gas price [k€/MWh]	0.06	
Electrolysis CAPEX [k€/MW]	1,125	Armstrong et al. (2022)
Hydrogen storage CAPEX [k€/tonne]	266.6	Armstrong et al. (2022)
Hydrogen hourly demand [tonne/hour]	38.5	
Interest rate [%]	7	
Electrolyzer operating bounds [% of capacity]	[10%, 100%]	
Storage operating bounds [% of capacity]	[5%, 95%]	

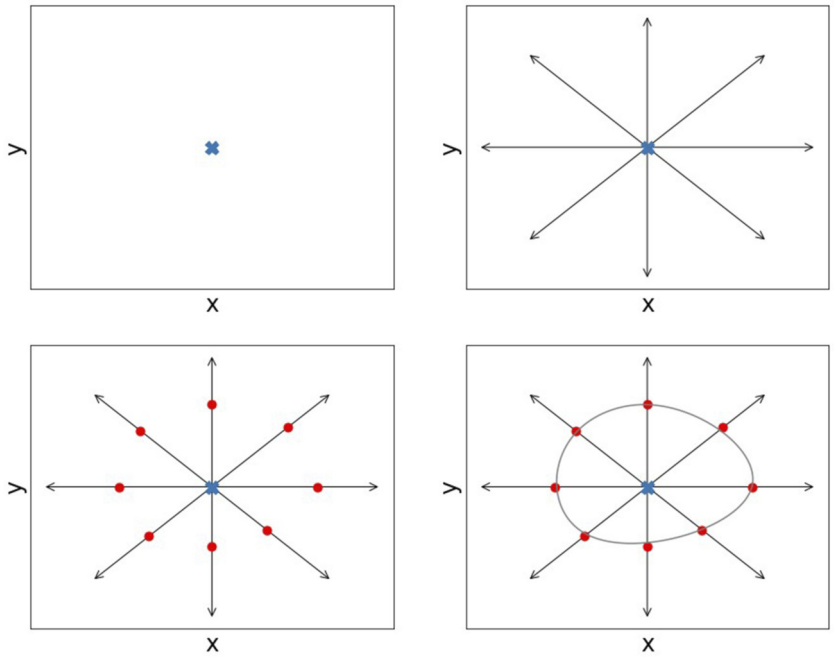

FIGURE 3
The steps of mapping near-optimal region.

After that, an optimization problem is solved for every θ_i. These problems are exactly like the ones derived in the model development section, except for a few modifications. In this problem, the purpose is to maximize the deviation of the optimization variables $[C, E]$ from the initial optimal values $[C^*, E^*]$. Therefore, the objective function is defined as Equation 16:

$$OF = k \tag{16}$$

In addition, the total system cost is an optimization variable rather than the objective function, see Equation 17.

$$TC = \sum_{g=1}^{g=G} \sum_{t=1}^{t=T} P_{g,t} \cdot MC_g + A_S \cdot C_S \cdot K_S + A_E \cdot C_E \cdot K_E \tag{17}$$

Finally, Equation 18 expresses that the total system cost is allowed to vary within an optimality gap ϵ from the stored objective function optimal value.

$$TC \leq (1 + \epsilon) \cdot OF^* \tag{18}$$

The final step in the mapping process is fitting a closed curve based on the solution of the optimization problems solved using the *splprep* function from the *scipy* library (Virtanen et al., 2020). This curve encompasses the near-optimal region points from the Scipy library. Figure 3 shows the four steps for mapping the near-optimal region.

In fact, the proposed near-optimal analysis complements classical parametric programming and local sensitivity analysis by shifting the focus from marginal responses around a single optimal solution to characterize the decision space that remains economically near-optimal. While parametric programming tracks how an optimal solution evolves under continuous parameter changes, and local sensitivity analysis quantifies marginal cost impacts, the near-optimal region approach identifies alternative capacity configurations that yield system costs within a predefined tolerance of the optimum. This is particularly relevant for linear energy system models, which often exhibit flat objective landscapes and multiple nearly equivalent optima. Throughout Section 4, the optimization results are illustrated through plots that show the evolution of the near-optimal regions under different power market settings. We have adopted certain values for the optimality gaps. The motivation behind the optimality gap value is mainly visual. In other words, we chose these values so that both readers and we can interpret the evolution of these regions with respect to certain parameters in a meaningful manner. This was a good balance: substantial variation of the single optimal point and small enough to consider them similar enough in cost to the optimal point.

4 Results and discussion

In this section, the optimization results are presented and discussed. Section 4.1 contains the results of a single optimization problem. In Section 4.2, the sensitivity of optimal storage and electrolysis capacities with respect to selected variables is portrayed. This was done by performing a series of optimization problems for a set of variable values.

4.1 Power system dynamics

In this section, we study the influence of flexibility on the power system. For a fair comparison, a base case is considered with no hydrogen storage, and a flexible case is considered with an

optimal storage capacity. To visualize the flexibility results, Figure 4 displays the time series for the first 2 weeks of the simulation year. Part a shows the renewable generation profile of solar and wind energy capacities. Part B portrays the residual demand, which is the additional energy that needs to be supplied to the system after accounting for renewable generation. A negative residual demand implies excess renewable energy generation and thus low energy prices. Part c shows the electricity consumption profiles of the electrolysis plants in the two cases. Note that in the absence of storage, the electrolysis capacity is lower because it is continually fully operating. When comparing parts b and c, a negative relation can be noticed between the energy consumption profile of the electrolyzer and the residual demand. This can be expected because lower residual demand means abundant cheap renewable energy; therefore, the electrolyzer operates at full capacity, and the excess hydrogen is stored for instances with negative residual demand. Part d shows the market price in the two cases. In the storage case, the market price can be described as more stable, as the electrolysis plant responds to the residual demand signal by shifting energy consumption to instances of low residual demand.

4.2 Design sensitivity

In this section, the influence of various problem parameters on the design and the optimal capacities of storage and electrolysis is studied. Rather than studying the variation of the optimal points, we examine the variation of the near-optimal regions. This method creates more coherent trends due to the shallow optimum of the problem. Additionally, it offers more in-depth insights.

4.2.1 CAPEX

In this subsection, the influence of storage and electrolysis CAPEX on the optimal capacities is studied. Figure 5 illustrates the variation of near-optimal regions as the CAPEX of storage and electrolysis vary between 50% and 150% of the original value. The first observation is that the near-optimal regions are larger in both cases for smaller CAPEX. This can be expected as smaller CAPEX implies a smaller contribution of investment costs to the overall costs. Thus, the optimum becomes even shallower. In addition, while the variation in storage CAPEX significantly influences the optimal storage capacity, it appears to have a much smaller effect on the optimal electrolysis capacity. In contrast, the variation of electrolysis CAPEX significantly influences both capacities. In other words, higher electrolysis capacity necessitates more storage, but it is not the same in the other direction. This is primarily because the cost of investing in storage is much smaller than the cost of investing in electrolysis, with a ratio of 1:25. The effect of this ratio can be recognized if we compare the variation of the levelized cost of hydrogen LCOH in both cases. While the increase in storage CAPEX raises the LCOH from 5.976 to 6.004 €/kg, the increase in electrolysis CAPEX raises the LCOH from 5.428 to 6.371 €/kg.

4.2.2 Renewables

Another essential factor that can influence the optimal hydrogen capacities is the renewable energy penetration in the power system. Figure 6 illustrates the variation of the regions as the additional capacities of solar and wind energy sources vary from 0 to 10 GW. Both graphs show a general trend of higher investment in flexibility for larger renewable energy capacities. Nonetheless, the increase in storage capacity is significantly larger than the increase in electrolysis capacity. Another similarity between the two graphs is that at + 10 GW, the electrolysis capacity declines, and the storage capacity increases. This is due to the high CAPEX of electrolysis. In addition, as renewable capacities increase, there will be more instances of excess renewable energy, allowing storage to be filled at a slower rate. Note that the electrolysis capacity required to directly supply the hydrogen demand is 1925 MW.

The primary difference between the two graphs is that the solar energy case favors a larger electrolysis capacity and substantially smaller storage capacity compared to the wind energy case. This is expected when comparing the generation profiles of both technologies. Although solar energy generation varies throughout the year, the main variation occurs on a daily basis. This sharp variation in abundant solar energy aligns the larger electrolysis capacity to utilize the peak and a smaller storage capacity, which is still sufficient to cover the intraday variation. On the other hand, a larger timescale of wind energy variation results in a larger storage capacity and a smaller electrolysis capacity. The additional renewable energy capacities reduce the average cost of energy generation in the system. Thus, the contribution of the investment cost to the total cost increases. In the initial case, the investment costs accounted for 16% of the total cost. This contribution increases to 32.1% in the case of +10 GW solar and 42.5% in the case of +10 GW wind. This high contribution leads to a sharper optimum and thus a smaller near-optimal region. The LCOH decreases from 5.991 €/kg in the initial case to 4.633 €/kg for +10 GW solar and 3.526 €/kg for +10 GW wind.

4.2.3 Carbon emitting generation

The carbon-emitting generation technologies, natural gas and coal, play a crucial role in the economics of the power system. Therefore, studying their influence on optimal investment should provide relevant insight. The natural gas price variation is considered because of its recent volatility. In addition, the carbon emission price is considered due to its impact on the generation costs and the merit order. Figure 7 shows the variation of the near-optimal regions for a set of natural gas and carbon emission prices.

The growth of storage and electrolysis capacities in response to increasing natural gas prices can be observed. However, the influence of the carbon emission price is not as straightforward as that of gas. To analyze this behavior, we will focus first on the variation of the regions' centers. This variation indicates that the system favors higher investment in flexibility assets for both smaller and larger carbon emission prices. In its essence, the flexibility would save costs as it allows for load shifts from high-price instances to low-price instances. If we refer to Figure 8, and more specifically to the merit order, we can observe a plateau in the merit order between the prices 120–150 €/kWh. This is because, for the initial natural gas and carbon emission prices, the generation costs of coal and some of the natural gas units are too close. Knowing that coal emits a much higher quantity of carbon dioxide per MWh, any increase or decrease in the carbon emission price leads to a gap between the coal and natural gas units, and therefore, to more potential benefits of

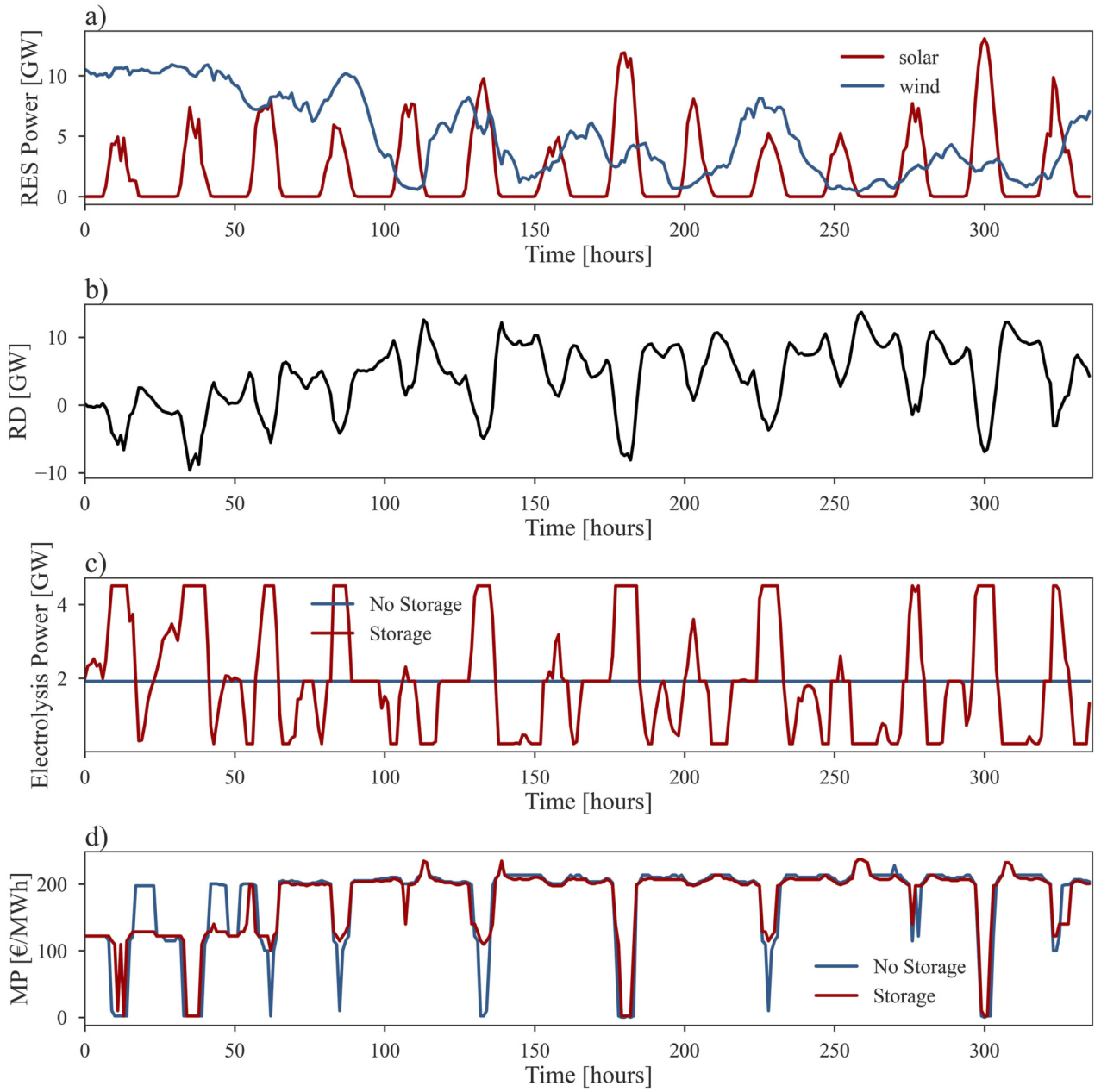

FIGURE 4
Two-week time-series of **(a)** solar and wind energy generation. **(b)** Residual demand. **(c)** Electrolysis power consumption. **(d)** Market price.

flexibility. A final note is that the LCOH is more sensitive to natural gas prices, as it varies from 4.339 to 6.908 €/kg, than to carbon emission prices, which vary from 5.098 to 6.789 €/kg.

4.3 Hydrogen demand flexibility

Based on the definition in Section 2.2.3, we study in this section the influence of hydrogen demand flexibility, or operational flexibility, on the optimal storage and electrolysis capacities.

Due to the small potential of flexibility benefits in the defined power system variables, a different case was considered for this section. The power system has been modified to match the PBL scenario of 2030 (PBL Netherlands Environmental Assessment Agency, 2022). The adjustments include higher renewable capacities, higher carbon emission prices, increased national demand, and the phasing out of coal plants. The results of the variation of the oversizing coefficient are depicted in Figure 9.

The complementary relationship between flexibility and storage is readily apparent. For both flexibility periods, the impact of demand flexibility on optimal storage capacity is more significant than its impact on optimal electrolysis capacity. A higher oversizing coefficient results in more flexible consumption, thereby reducing the need for hydrogen storage. In addition, the influence of the

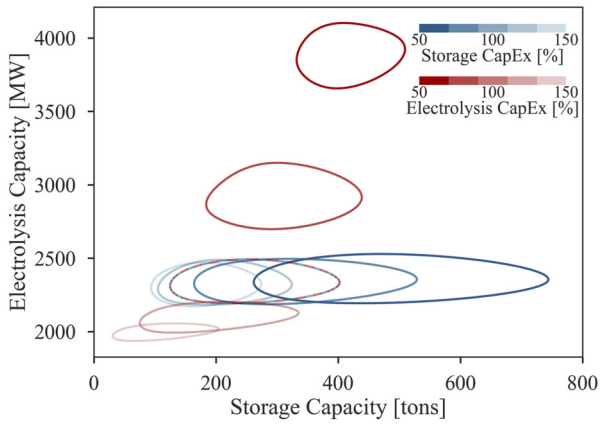

FIGURE 5
Near-optimal regions for different CAPEX for *epsilon* = 0.05%.

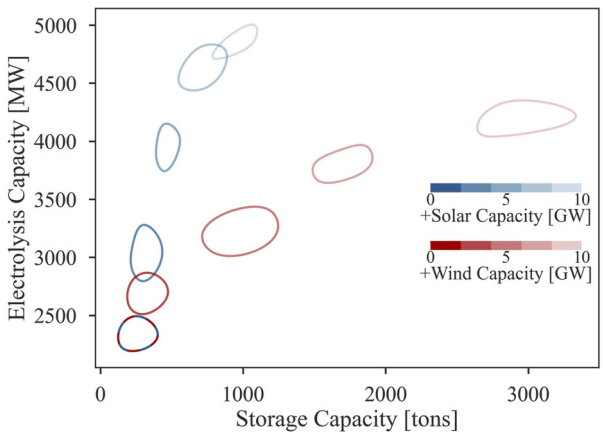

FIGURE 6
Near-optimal regions for different renewable energy capacities for *epsilon* = 0.05%.

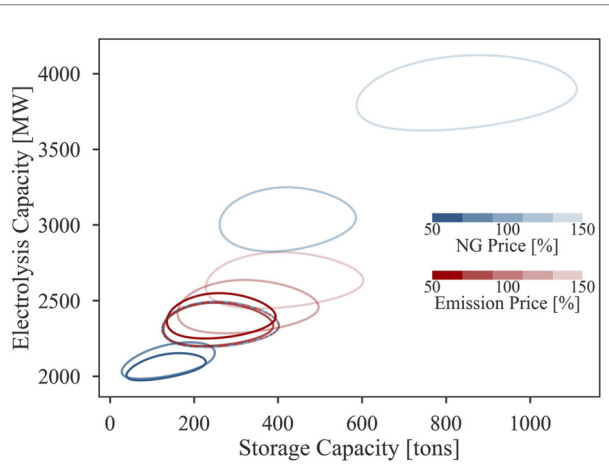

FIGURE 7
The variation of near-optimal regions for different natural gas and carbon emission prices for *epsilon* = 0.1%.

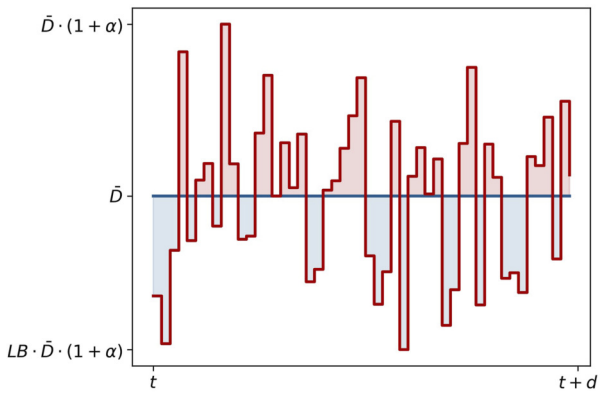

FIGURE 8
A comparison of the fixed demand and a variable demand profile where the two shaded areas are equal due to the quota constraint.

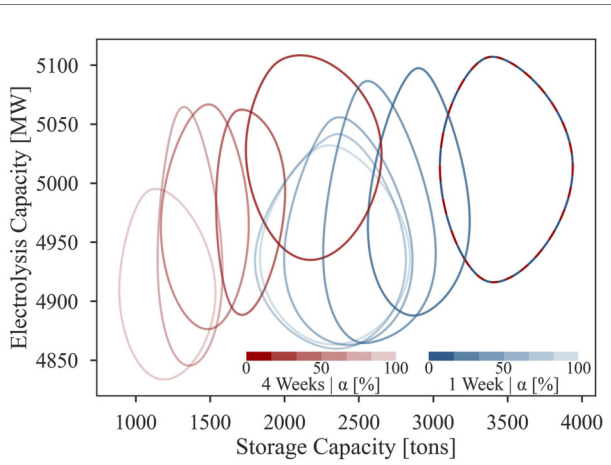

FIGURE 9
The variation of near-optimal regions vs. oversizing coefficient with flexibility period of 1 month and 1 week for epsilon = 0.1%.

flexibility period can be analyzed by comparing the evolution of the near-optimal regions for the 1-week and 1-month periods. The impact of the oversizing coefficient in the 1-week period plateaus for values greater than 50%. On the other hand, for a monthly flexibility period, larger alphas result in a significantly smaller optimal storage capacity and a slightly smaller electrolysis capacity. The operational flexibility also has an impact on the LCOH. For an oversizing coefficient of 0%, or no operational flexibility, the LCOH in this simulation is 4.177 €/kg. In the 1-week case, this value drops to 4.065 €/kg for a 60% oversizing coefficient, and 4.058 €/kg for a 100% oversizing coefficient. In contrast, the monthly-case results in a drop to 3.866 €/kg for a 60% oversizing coefficient, and 3.804 €/kg for a 100% oversizing coefficient.

5 Conclusion

This paper presents a novel approach to analyzing and gaining insights into the influence of power system variables on

optimal investment decisions in flexibility facilities. The scenario of hydrogen demand for a decarbonized steel industry was considered. A model that combines the power system element and the hydrogen flow element was built for this analysis. Afterward, the variation of optimal capacities with respect to selected problem variables was studied. Nevertheless, rather than interpreting the behavior of point optima, the behavior of near-optimal regions was studied. This enabled a better understanding of the optimal investment spaces.

In order to map the near-optimal regions, a novel method was employed. This method utilized the convexity property of the linear optimization problem to identify a number of points on a contour curve with a predefined optimality gap. The points were then used to fit the boundary of the near-optimal region. The analysis showed a shallow optimum with a relatively large near-optimal region for small gaps.

Regarding the CAPEX of the hydrogen facilities, the results indicated high sensitivity to the electrolysis CAPEX and low sensitivity to the storage CAPEX. It has been concluded that a larger electrolysis capacity necessitates a larger storage capacity, but not *vice versa*.

The optimal storage and electrolysis capacities reacted distinctly to additional solar and wind installations. The sharp intraday variation of solar generation favors higher investments in electrolysis and lower investments in storage when compared to wind energy. Besides, the simulations showed a clear relationship between natural gas prices and the capacities of hydrogen facilities. However, the impact of carbon emission prices on these capacities is not as simple; the investment in flexibility is always aligned with the gap between the total generation costs of natural gas and coal units.

In addition, a hydrogen demand flexibility model is introduced. It is based on the oversizing of the reduction plant and a fixed quota of hydrogen consumption over a period of time. The simulation results show a complementary relationship between the oversizing coefficient α and the optimal storage capacity.

The work presented in this paper paves the way for more advanced studies. Building on the developed model and the method of near-optimal region mapping, an investment optimization over a project lifetime with a varying power system can be achieved. In addition, the interactions among several large flexible consumers and the power system can be studied.

In a broader context, this work highlights the importance of studying the evolution of the solution space, rather than focusing solely on the optimal point, across different power system conditions. This calls for further research into the implications of market design and policy on optimal hydrogen investments. The size of the near-optimal region can provide additional motivation to investigate the trade-offs among different investment options.

Data availability statement

The raw data supporting the conclusions of this article will be made available by the authors, without undue reservation.

Author contributions

AN: Conceptualization, Methodology, Visualization, Writing – original draft, Writing – review and editing. RV: Methodology, Supervision, Validation, Writing – review and editing. LD: Methodology, Supervision, Writing – review and editing.

Funding

The author(s) declared that financial support was received for this work and/or its publication. This work is part of the RELEASE project, funded by the Dutch Research Council (NWO) (project number 17621). The position of LD is sponsored by the Dutch government agency EBN ((http://www.ebn.nl)www.ebn.nl).

Conflict of interest

The author(s) declared that this work was conducted in the absence of any commercial or financial relationships that could be construed as a potential conflict of interest.

Generative AI statement

The author(s) declared that generative AI was not used in the creation of this manuscript.

Any alternative text (alt text) provided alongside figures in this article has been generated by Frontiers with the support of artificial intelligence and reasonable efforts have been made to ensure accuracy, including review by the authors wherever possible. If you identify any issues, please contact us.

Publisher's note

References

Angizeh, F., Parvania, M., Fotuhi-Firuzabad, M., and Rajabi-Ghahnavieh, A. (2019). Flexibility scheduling for large customers. *IEEE Trans. Smart Grid* 10 (1), 371–379. doi:10.1109/tsg.2017.2739482

Armstrong, R., Chiang, Y.-M., and Gruenspecht, H. (2022). *The future of energy storage: an interdisciplinary MIT study*. Massachusetts Institute of Technology.

Boldrini, A., Koolen, D., Crijns-Graus, W., and Broek, M. V. D. (2022). "The demand response potential of a hydrogen-based iron and steel plant," in *2022 18th International Conference on the European Energy Market (EEM)*, 1–6. doi:10.1109/EEM54602.2022.9921013

Corbie, J. (2024). *Analyse van de gevolgen van het Energieakkoord vor de Nederlandse elektriciteitmarkt*. TU Delft. PhD thesis.

ENTSO-E (2023). *Entso-e transparency platform*.

Gurobi Optimization, LLC. (2023). *Gurobi optimizer reference manual*.

Grochowicz, A., van Greevenbroek, K., Benth, F. E., and Zeyringer, M. (2023). Intersecting near-optimal spaces: european power systems with more resilience to weather variability. *Energy Econ.* 118 (June 2022), 106496. doi:10.1016/j.eneco.2022.106496

Haoxin, D., Qiyuan, D., Chaojie, L., Nian, L., Zhang, W., Hu, M., et al. (2025). A comprehensive review on renewable power-to-green hydrogen-to-power systems: green hydrogen production, transportation, storage, re-electrification and safety. *Appl. Energy* 390, 125821. doi:10.1016/j.apenergy.2025.125821

Jia, W., Ding, T., and He, Y. (2026). Synergistic integration of green hydrogen in renewable power systems: a comprehensive review of key technologies, research landscape, and future perspectives. *Renew. Sustain. Energy Rev.* 226 (PD), 116375. doi:10.1016/j.rser.2025.116375

Krüger, A., Andersson, J., Grönkvist, S., and Cornell, A. (2020). Integration of water electrolysis for fossil-free steel production *Int. J. Hydrogen Energy* 45 55. 29966–29977. doi:10.1016/j.ijhydene.2020.08.116

Lombardi, F., Pickering, B., Colombo, E., and Pfenninger, S. (2020). Policy decision support for renewables deployment through spatially explicit practically optimal alternatives. *Joule* 4 (10), 2185–2207. doi:10.1016/j.joule.2020.08.002

Lombardi, F., Pickering, B., and Pfenninger, S. (2023). What is redundant and what is not? Computational trade-offs in modelling to generate alternatives for energy infrastructure deployment. *Appl. Energy* 339 (February), 121002. doi:10.1016/j.apenergy.2023.121002

Neumann, F., and Brown, T. (2021). The near-optimal feasible space of a renewable power system model. *Electr. Power Syst. Res.* 190 (September 2020), 106690. doi:10.1016/j.epsr.2020.106690

Pandzic, H., Wang, Y., Qiu, T., Dvorkin, Y., and Kirschen, D. S. (2015). Near-optimal method for siting and sizing of distributed storage in a transmission network. *IEEE Trans. Power Syst.* 30 (5), 2288–2300. doi:10.1109/tpwrs.2014.2364257

Papadaskalopoulos, D., Moreira, R., Strbac, G., Pudjianto, D., Djapic, P., Teng, F., et al. (2018). Quantifying the potential economic benefits of flexible industrial demand in the european power system. *IEEE Trans. Industrial Inf.* 14 (11), 5123–5132. doi:10.1109/tii.2018.2811734

PBL Netherlands Environmental Assessment Agency (2022). *Klimaat-en energieverkenning 2022*.

Pedersen, T. T., Victoria, M., Rasmussen, M. G., and Andresen, G. B. (2021). "Exploring flexibility of near-optimal solutions to highly renewable energy systems," in *Conference Record of the IEEE Photovoltaic Specialists Conference*, 387–391.

Sofana Reka, S., and Ramesh, V. (2016). Industrial demand side response modelling in smart grid using stochastic optimisation considering refinery process. *Energy Build.* 127, 84–94. doi:10.1016/j.enbuild.2016.05.070

Teo, T. T., Logenthiran, T., Woo, W. L., and Abidi, K. (2018). "Near-optimal day-ahead scheduling of energy storage system in grid-connected microgrid," in *International Conference on Innovative Smart Grid Technologies, ISGT Asia 2018*, 1257–1261.

Tsay, C., Kumar, A., Flores-Cerrillo, J., and Baldea, M. (2019). Optimal demand response scheduling of an industrial air separation unit using data-driven dynamic models. *Comput. Chem. Eng.* 126, 22–34. doi:10.1016/j.compchemeng.2019.03.022

Varela, C., Mostafa, M., and Zondervan, E. (2021). Modeling alkaline water electrolysis for power-to-x applications: a scheduling approach. *Int. J. Hydrogen Energy* 46 (14), 9303–9313. doi:10.1016/j.ijhydene.2020.12.111

Virtanen, P., Gommers, R., Oliphant, T. E., Haberland, M., Reddy, T., Cournapeau, D., et al. (2020). SciPy 1.0: fundamental algorithms for scientific computing in python. *Nat. Methods* 17, 261–272. doi:10.1038/s41592-019-0686-2

Voll, P., Jennings, M., Hennen, M., Shah, N., and Bardow, A. (2015). The optimum is not enough: a near-optimal solution paradigm for energy systems synthesis. *Energy* 82, 446–456. doi:10.1016/j.energy.2015.01.055

Zhang, X., Hug, G., Kolter, Z., and Harjunkoski, I. (2016). "Computational approaches for efficient scheduling of steel plants as demand response resource," in *19th Power Systems Computation Conference, PSCC 2016*.

Nomenclature

$()_E$	of electrolysis
$()_g$	of generation unit g
$()_S$	of storage
$()_t$	at hour t
$()_{res}$	of renewable energy generation
$\boldsymbol{\alpha}$	Oversizing coefficient [%]
$\bar{\boldsymbol{D}}_{H_2}$	Non-flexible hydrogen consumption [tonne/hour]
$\boldsymbol{\eta}_E$	Electrolysis efficiency [tonne/MWh]
$\boldsymbol{\eta}_S$	Storage efficiency [%]
$\boldsymbol{A}$	Annuity factor
$\boldsymbol{C}$	CAPEX [k€/MW]
$\boldsymbol{CF}_t$	Hourly capacity factor of renewable generation [%]
$\boldsymbol{d}$	Flexibility period [hour]
$\boldsymbol{D}_E$	National electricity demand [MW]
$\boldsymbol{D}_{H_2,t}$	Flexible hydrogen consumption [tonne/hour]
$\boldsymbol{F}_{H_2,in}$	Hydrogen inflow rate to the storage tank [tonne/hour]
$\boldsymbol{F}_{H_2,out}$	Hydrogen outflow rate of the storage tank [tonne/hour]
$\boldsymbol{G}_{H_2}$	Hydrogen gas synthesis [tonne/hour]
$\boldsymbol{K}$	Capacity [MW]
$\boldsymbol{LB}$	Lower bound [%]
$\boldsymbol{MC}$	Marginal cost of generation [k€/MWh]
$\boldsymbol{OF}$	Objective function [k€
$\boldsymbol{P}$	Power [MW]
$\boldsymbol{UB}$	Upper bound [%]
$\boldsymbol{P}_{s,t}$	Hydrogen compression power [MW]